Facies (2005) 51: 135–145
DOI 10.1007/s10347-005-0062-9

ORIGINAL ARTICLE

Günter Landmann · Stephan Kempe

Annual deposition signal versus lake dynamics: Microprobe analysis of Lake Van (Turkey) sediments reveals missing varves in the period 11.2–10.2 ka BP

Received: 23 December 2004 / Accepted: 10 March 2005 / Published online: 24 June 2005

Abstract Microprobe measurements revealed changes of elemental concentrations along thin-section profiles of laminated Lake Van sediments. Results show pronounced variations, interpreted as seasonal cycles, thus allowing a new varve count based on alternating Ca and Si peaks. Compared with previous optical counts, the new record adds 170 years and places the investigated interval at 11.2–10.2 ka BP. The microprobe data reveal unusual Mg concentrations between 11.2 and 10.7 ka BP. These are caused by diagenetic magnesite and protodolomite, thought to be indicative of a lake-level regression and evaporative conditions causing the Mg content of the lake water to rise to critical levels. The dry phase ended with a transgression that started at around 10.7 ka BP and brought about a meromictic phase which weakened the climate-induced seasonal deposition signal. Both the diagenetic mineral formation and the mixing behavior of the lake decreased the grey scale value differences of the annual deposition signal, which had led to underestimation of years when varves were counted optically. Similar processes may have occurred in the evolution of Lake Lisan which would explain the marked differences between optical laminae counting and radiocarbon dating observed by other authors.

Keywords Lake Van · Varve chronology · Varve formation · Diagenesis · Microprobe

Introduction

Lake Van is located in the highlands of Eastern Anatolia, Turkey. With a maximum depth of 451 m, a surface of 3522 km^2 and a volume of 576 km^3, it is the fourth largest closed lake on Earth. The water of the lake is highly alkaline with a pH of 9.8, an alkalinity of 153 meq l^{-1} and a salinity of 22 per mill. It is therefore the largest soda lake on Earth. The lake's sediments are composed of calcareous, laminated mud, taken to be annual varves. The sediment record is interrupted by up to 12 volcanic ash layers, turbidites, and slumps. These sediments were sampled (Fig. 1) with nine cores in 1974 (Degens and Kurtmann 1978) and with 10 additional cores in 1990 (Landmann et al. 1996a). The cores can be easily correlated throughout the central basin using the ash layers and certain marker layers, assuring the completeness of the record.

Three varve chronologies exist of Lake Van, established by different methods:

1. In the combined 1974 cores of St. 14 (for the upper part of the record) and St. 3 (for the lower part of the record), Kempe (1977) counted 10,420 varves macroscopically on the smoothened cutting planes of the sediment core. Difficulties were associated with the topmost section due to the compression during the coring process. Therefore, the first ash layer was assumed to be the year AD 1441, the date of the most recent eruption of the Nemrut volcano on the eastern side of the lake.
2. From the core K10 taken in 1990, Landmann (1996) prepared thin-sections and polished slabs from one half of the undisturbed core. Varve counts and annual sediment accumulation rates were established by automated processing of light absorption curves obtained by scanning the polished slabs, combined with an optical identification of laminae at a 10–20-fold on-screen magnification. Where deviations between the two automated counts and the optical counts occurred, sections were additionally inspected with a microscope (Landmann et al. 1996a).
3. From the other half of core K10, another set of thin-sections was prepared by Lemcke (1996). Varves were counted with a microscope, using normal and polarized light to differentiate between the organic or carbonate-rich layers which mark seasons.

The counting results show that the average sedimentation rate in the central basin of the lake amounts to 0.5 mm a^{-1}. The cores cover roughly 15,000 years of lake history, presenting one of the longest uninterrupted varve records

G. Landmann (✉) · S. Kempe
TU Darmstadt, Institut für Angewandte Geowissenschaften,
Schnittspahnstr. 9,
64287 Darmstadt, Germany
e-mail: guenter.landmann@donnerstrasse.de

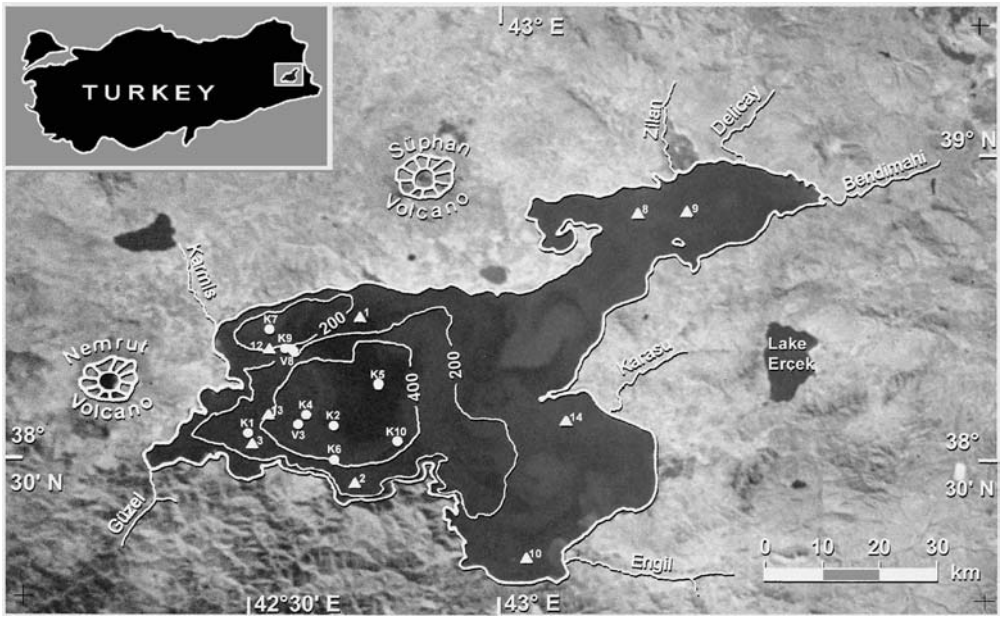

Fig. 1 Map of Lake Van with the location of cores taken in 1974 (*triangles*) and in 1990 (*solid circles*). Map background based on a photo taken during the Challenger 6 space mission in October 1984. Carbonate precipitation is visible as whitings on lake surface

available. Changes in sediment chemistry and deposition rates reveal rapid and pronounced lake-level fluctuations, thus yielding important information on palaeoclimate in a region not directly influenced by the North-Atlantic climate regime, making the lake a unique complement to the European palaeoclimate records.

Significant deviations between the St.14/3 and the K10 counts occur in the upper part of the record and can be attributed to the strong compression and loss of sediment encountered in core St. 14 (Fig. 2; Landmann et al. 1996b). Additionally, for the period 4–14*[1] ka BP, the slope of the correlation curve is slightly lower than 1:1, suggesting that some varves were missed in the macroscopic counting process by Kempe (1977). The chronologies of Lemcke (1996) and Landmann (1996) correspond well among each other with a maximum deviation of less than 2.4%. In the period 11–10.2* ka BP, all three chronologies deliver similar number of varves, showing that the individual counting error is rather low (Fig. 2).

To test the Lake Van record with independent chronologies, it was compared with snow accumulation and delta^{18}O records of the Greenland ice cores (Fig. 3; Landmann and Kempe 2002). The chronologies of the GRIP and GISP2 records differ slightly among each other but are now accepted as the standard chronology to date the abrupt temperature changes which structure the Late Pleistocene palaeoclimate. The 8.2 ka Event, expressed in the Lake Van record by a lake-level minimum and slightly higher sediment deposition rates, seems to occur in phase with the ice record. In the period 11–10* ka BP, the deposition rate of Lake Van was exceptionally high and sediment chemistry indicates a lake-level minimum. The length of Late Pleistocene chronozones defined for Greenland ice cores are very similar in duration to chronozone duration in the varve record,

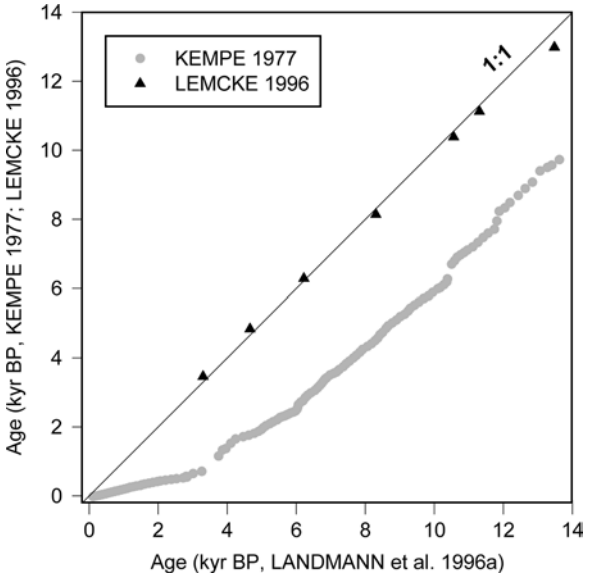

Fig. 2 Comparison of the three Lake Van varve chronologies prepared by Kempe (1977), Landmann (1996), and Lemcke (1996). Data points below 1:1 gradient (*line*) indicate ages younger than varve count prepared by Landmann and vice versa

but the varve ages are 600–700 years younger for the termination of the Younger Dryas (YD) than in Greenland (Alley et al. 1993; Grootes et al. 1993; Landmann and Kempe 2002). At around 15 ka BP the varves fade out completely.

To date, coring could not penetrate a hard layer underlying the postglacial varved sediments. Its texture, mineralogy, and geochemistry is strikingly different from the rest of the sediment column. It lacks lamination, contains large rounded pumice pieces and ooliths and has an elevated dolomite content. This layer is thought to document a drying-up of the lake (Landmann et al. 1996b). Low lake levels or desiccation at around 15 ka BP were also reported

[1] Dates marked by an asterisk are based on the old chronology given by Landmann et al. (1996a)

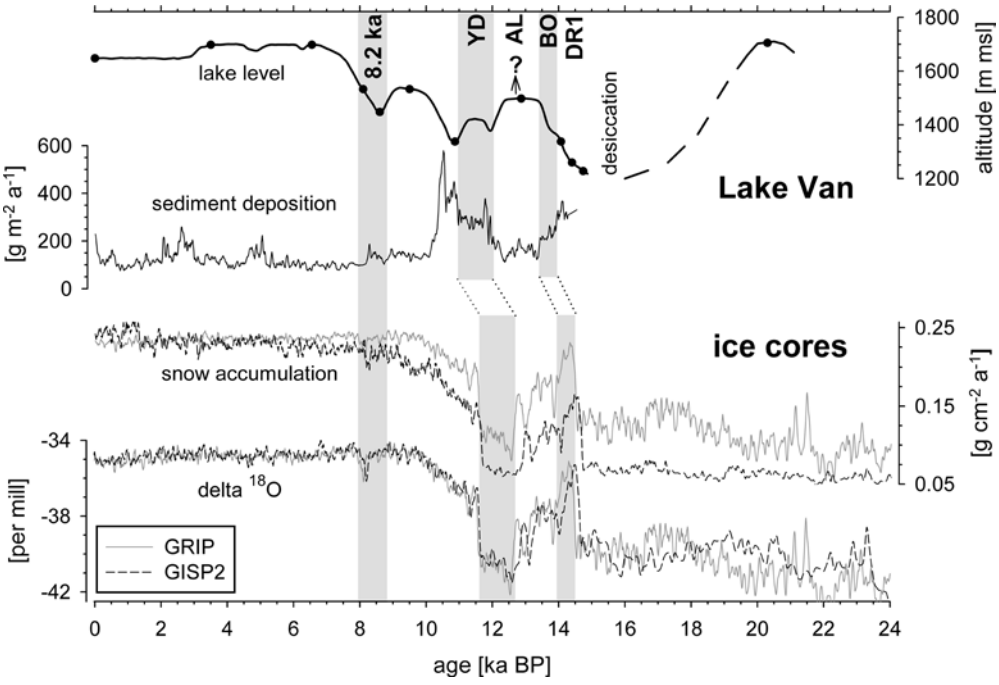

Fig. 3 Comparison between Lake Van and Greenland ice core records. With the exception of the lake-level curve, all data were interpolated to annual resolution, reduced by calculating averages for 11 years and smoothened by a running mean of five values. Lake Van ages based on Landmann (1996); the ice core data are from Alley et al. (1993) and Grootes et al. (1993)

from Lake Lisan, precursor of the Dead Sea (Neev and Emery 1967, 1995), and from Lake Viktoria, East Africa (Talbot and Lærdal 2000). A pronounced lowstand lasting about 1000 years occurred between ca. 15 and 14 ka BP at Lake Estancia, central New Mexico, USA (Allen and Anderson 2000).

Older deposits are, however, found in terraces around Lake Van. The sediment outcrop at the River Engil, 35 m above the present lake level, is also mostly laminated and was used to establish a floating varve chronology of 606 years (Kempe et al. 2002). This chronology was fixed by ^{14}C-dates to the period 20.7–20.1 ka BP, thus indicating a highstand of Lake Van during the Last Glacial Maximum.

High-resolution archives are important to understand climate instability. The missing agreement of the varve counts with the Greenland ice cores in the period after the YD termination leads to the suspicion that optical counting has missed the annual signal in some sections of the sediment record. The duration of the Younger Dryas stage at Lake Van (1120 years) is in good correspondence with lacustrine records of Meerfelder Maar, Germany, Hämelsee, Germany, Lake Gościąż, Poland and Lake Perespilno, Poland (1100–1150 years; Brauer et al. 1999; Litt et al. 2001). But floating varve chronologies of these central European lakes date the YD termination to 11,480–11,590 BP.

In 11–10* ka BP, the sediment deposition rate at Lake Van was exceptionally high, with significant decadal oscillations and a pronounced maximum at 10.5* ka BP. This feature is interpreted to represent a lake-level minimum followed by a rapid transgression caused by enhanced precipitation and melting of mountain glaciers (Landmann et al. 1996a, b). Transgressive lake phases are particularly suitable to establish density stratification in the water column since riverine freshwater will overlay the saline lake water of higher density. A meromictic stage is indicated by a conspicuous layer deposited at around 10.5* ka BP. It consists of several thick dark-brown varves with unusually high organic carbon content. Biomarker analyses revealed high concentration of long-chained alkenones, most likely due to intense plankton blooms caused by an eutrophication event which was triggered by complete overturn of the lake following a longer stagnation period (Thiel et al. 1997).

The changed lake dynamics in 11–10* ka BP may have affected varve formation. Therefore, we applied microprobe analysis to the thin-sections of this important period in order to study the deposition processes of the lake in more detail and to improve the varve counting by detecting the seasonal changes in the chemical composition of the sediments.

Materials and methods

A Cameca SX 50 microprobe equipped with four spectrometers was used for a continuous line scan covering the period 11,012–10,249* a BP of the chronology prepared by Landmann (1996). A beam size of 50 µm was used to resolve the average annual sediment accumulation at Lake Van (0.5 mm a^{-1}) with at least 10 analyses per year. A higher resolution enhances measurement variation since sediment and resin are not homogenously distributed on the thin-sections. Best results were obtained using a voltage of 20 kV and a current of 20 nA for the beam with a counting time of 500 ms. The measured section covers 522.9 mm distributed on 12 thin-sections (see Landmann et al. 1996a for thin-section preparation).

The measured section was subdivided in 19 profiles with lengths between 18.9 and 37.4 mm; this always allowed a profile direction perpendicular to the lamination. To have

an unbroken record, start and end points of subsequent line scans were correlated. After marking them, thin-sections were photographed and sputtered with carbon. The elements Si, Ca, Mg, Al, K, Fe, Na, S, Ti, and P were analyzed but the signal to noise ratio of the elements S, Ti, and P was too low to allow meaningful interpretation. However, the remaining seven elements are the major components of Lake Van sediment. Up to three parallel line scans with all elements were done to minimize analytical errors and to enhance statistical accuracy of the measurements.

Signal intensity of microprobe analyses, in the way conducted here, is a measure of element concentration within a resin-hardened sediment surface of about 2000 μm^2. It depends not only on careful calibration of the electron beam but also on the physical and structural state of the sample, such as sediment porosity or roughness of the sample surface. For example, small dots of a felt-tip pen used to mark the start and end of the profile on the sample reduce peak intensities by about 99%. Low counts caused by fissures or other relicts of preparation were deleted from the data sets resulting in a total data gap of 41.8 mm. To reduce and smoothen data for quantification of a general trend, mean values were calculated for each profile, resulting in an average resolution of 40 years. These mean values were standardized by setting the sum of counts for all seven elements to 100%. This procedure excludes differences in signal intensity attributed to porosity variations therefore enhancing comparability of subsequent line scan sections.

Comparison between XRF and microprobe analyses

An attempt was made to quantify microprobe measurements by X-ray fluorescence (XRF) analyses. Only two XRF-analyses are available within the investigated

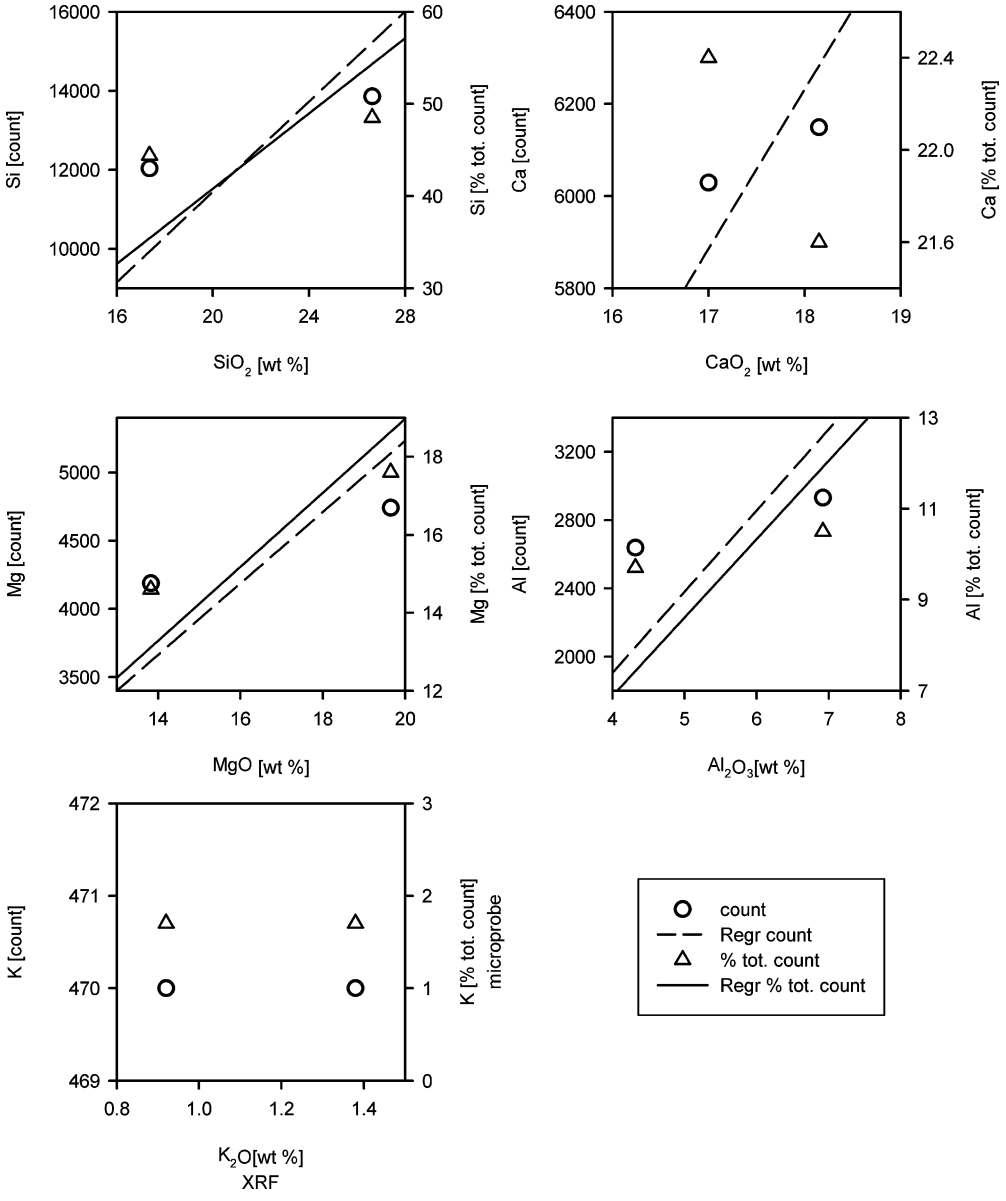

Fig. 4 Concentrations of Si, Ca, Mg, Al, and K in Lake Van sediment in the period 10.9–10.5* ka BP. The elements were quantified by X-ray fluorescence (*x*-axis) and by microprobe (*y*-axis). Results of microprobe analyses are plotted as original counts (*circles*) and percentage of total counts (*triangles*). Also given are linear regressions passing through data origin

time window (Landmann et al. 1996a). They were made on samples taken from core K6 and average 5–5.5 cm of the sediment column. Age was determined by detailed correlation of core K6 with the dated core K10, resulting in a mean age of 10,590* and 10,875* a BP of the two samples, respectively. Results of the two XRF-analyses were plotted *versus* microprobe data extracted from the corresponding section as average data of 5–5.5 cm profile, *versus* counts as well as *versus* percentage of total counts (% tot. count; Fig. 4).

There is a positive correlation between microprobe and XRF-measurements for the major elements Si, Ca, Mg, and Al, but their slope is always less than the slope of the regression passing through the origin. This may be due either to a nonlinear relation between the two measurements, or to a high level of background noise for microprobe analyses. The latter is, however, not very likely because measurements of pure resin yielded 20–200 counts only. In case of Ca, a positive correlation is present only between the XRF data and microprobe counts (Fig. 4) but not between XRF data and % of total counts; the small difference of 120 counts between the two analyses disappears when the percentage of total counts is calculated. Elements with low concentration show no (K) or negative regression (Na, Fe; not shown). For Na, comparable results cannot be expected since microprobe samples contain water-soluble salts while XRF-samples were pre-washed. Overall, results based on the comparison of only two samples are too vague to establish a reliable transfer function between the different methods.

Element variation of sediment composition within the period 11–10.25* ka BP and its climate interpretation

Results of microprobe analyses for all elements as well as the standard deviation of repeated measurements are plotted *versus* age (Fig. 5). From 11 to 10.6* ka BP, the concentrations of Si and Al decrease while the Mg content is exceptionally high. Low Al values can be taken as an indication of a reduced river input that in turn leads to a lake-level drop. Increasing salinity caused a shift of carbonate mineral equilibria to a preferential formation of Mg-carbonates. Magnesite and protodolomite were found in deposits of this period (Landmann et al. 1996b). The high number of total counts from 10.9 to 10.7* ka BP (Fig. 5, top) indicates a high sediment density and low porosity, suggesting that this Mg-carbonate formed at least partially during early diagenesis.

From 10.6 to 10.4* ka BP, the temporal variation of all elements is high. Concentrations of Al, K, and Na are elevated, while Mg and Ca show an opposing pattern. Si concentration remains low until 10.5 ka BP but increases strongly afterwards. Unfortunately, there are large standard deviations between multiple measurements within this period, complicating a detailed interpretation. Over the entire time window, there is a relevant positive correlation between Al and K ($r = 0.838$) and a negative correlation between Al and Mg ($r = -0.744$).

Inputs of dissolved matter to closed lakes either accumulate in the lake water or, if solubility of certain minerals is exceeded, precipitate. Residence times of specific components (defined as mean lake water concentration multiplied by lake volume divided by mean river concentration multiplied by annual river flux; e.g., Langbein 1961) help to interpret the microprobe data. Together with average deposition rates, elemental residence times for Lake Van calculated by Kempe (1977) and Reimer (1995) allow to estimate mass budgets (Table 1).

Average annual deposition of Ca, Mg, and K is approximately balanced by river input with a recent flux rate and the current water composition (compare columns 3 and 4 in Table 1), while Si and Fe may indicate additional eolian inputs or increased river inputs in the past. Due to the high alkalinity of Lake Van (pH 9.8), Ca concentration is kept at a very low level (4 mg l^{-1}) leading to a short residence time. Highest residence time is obtained for Na which has a high input surplus. K and Mg also accumulate in the lake water. Variations of these elements in the sediment

Table 1 Mass budgets for certain elements for Lake Van

Element	Residence time (a)	River flux (g m^{-2} a^{-1})	Deposition	
			Average (g m^{-2} a^{-1})	11–10.2* ka BP (g m^{-2} a^{-1})
Si	61	6.32	22.80	40.20
Ca	31	21.12	23.98	49.11
Mg	2080	8.67	9.01	39.47
K	30,800	2.28	1.72	3.73
Na	109,600	11.86	1.19	2.19
Fe	192	0.03	4.00	8.78
Al	–	–	5.38	11.63

Note. Data of residence time and river flux were taken from Reimer (1995). River flux corresponds to minimum values since it disregards sublacustrine sources estimated to an additional 17%. Deposition of different elements was calculated using a deposition rate of 164 g m^{-2} a^{-1} (mean of the core K10; see Fig. 3) and an average composition of 45 XRF-analyses on laminated sediments or by a deposition rate of 391 g m^{-2} a^{-1} (mean of the period 11–10.2* ka BP) and an average of two XRF samples from this period (Landmann 1996). Note the over proportional strong increase of Mg concentration in the period 11–10.2* ka BP.

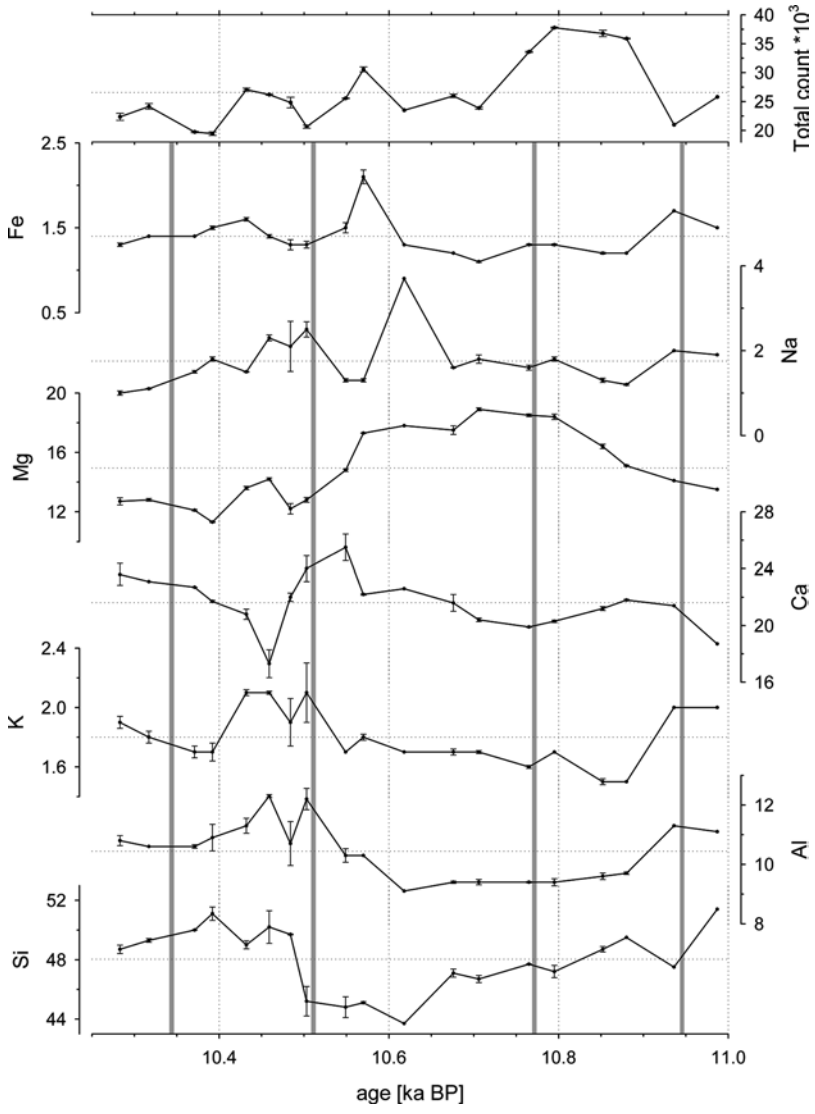

Fig. 5 Number of total counts (top) and concentration of seven major elements measured by microprobe. The *x*-axis presents the age according to the varve chronology prepared by Landmann (1996). Element concentration is given as a percentage of total counts. Error bars indicate standard deviation of multiple measurements. The shaded vertical lines indicate the period of samples presented in Fig. 6

column may, therefore, indicate precipitation due to surpassing of mineral solubility during pronounced lake-level regressions, while the variations of elements with a short residence time (Ca, Si) more likely reflect changes in river flux.

Based on these considerations, we have to conclude that the lake-level regression comes to an end at 10.6* ka BP and that river fluxes and lake level started to increase again, as indicated by the increase of Si, Al, and Ca as well as by decreasing Mg concentration (Fig. 5). Ca rises more quickly than Si between 10.6 and 10.5* ka BP, a fact that may reflect the accumulation of nearshore, Ca-enriched deposits. High K and Na concentrations in this period point to a pronounced lake-level rise beginning from a relatively low water stand. Al also augments faster than Si, suggesting increased river influx but low diatom productivity. Diatoms are a significant source for amorphous Si in the sediment which reaches, on average, 15% of weight, pointing to the importance of diatoms in primary production (Reimer 1995). The increase of biogenic opal concentration at 10.5* ka BP gives evidence of enhanced nutrient supply and improved salinity conditions for diatoms therefore confirming the continuation of the transgression.

Seasonal deposition sequence and varve chronology

The formation of varves in Lake Van is controlled by the pronounced seasonality of the continental climate in Eastern Anatolia; warm, dry summers are followed by long, cold winters. Prevailing south-westerly winds from the Mediterranean bring winter and spring precipitation. Most precipitation falls in March and April, simultaneously with the start of snow melt. This causes a peak in river runoff from April to June, triggering a pronounced rise of the lake level. A freshwater layer is formed, enriched in Ca compared to the saltier and therefore heavier lake water (salinity: 22 per mill). The continuous mixing of the Ca-rich river water and the highly alkaline lake water causes spontaneous precipitation of $CaCO_3$ either in form of local plume-like whitings near river mouths or throughout the lake at its surface. Satellite pictures show that the

lake-wide whitings are most pronounced in late summer when evaporation has concentrated the surface water (Landmann 1996). Dust storms occur and may occasionally contribute terrigenous material to the lake in summer (as observed during our expedition in 1990). Even though the winters in Eastern Anatolia are severe, the lake never freezes due to its high salinity; in fact, it serves as a heat reserve to the lake coast. In winter, the late summer layer cools and convection sets in, partially renewing the hypolimnion. These are the main seasonal features determining the laminated nature of the sediments in the lake. It is interesting that the sediments are not bioturbated even though bottom waters seem to contain oxygen in certain periods (as for example today); the true reason for the missing bioturbation seems to be the absence of macro-benthos which apparently has not adapted to the high alkalinities and pH of the lake.

In spring, the rivers bring an increased load of terrigenous and hence Al-rich material which forms a dark brown lamina. Next, a carbonate-rich layer forms during late summer due to continued evaporation and mixing of Ca-rich river water and alkaline lake water. A third layer, with an even stronger color contrast to the white carbonate forms in

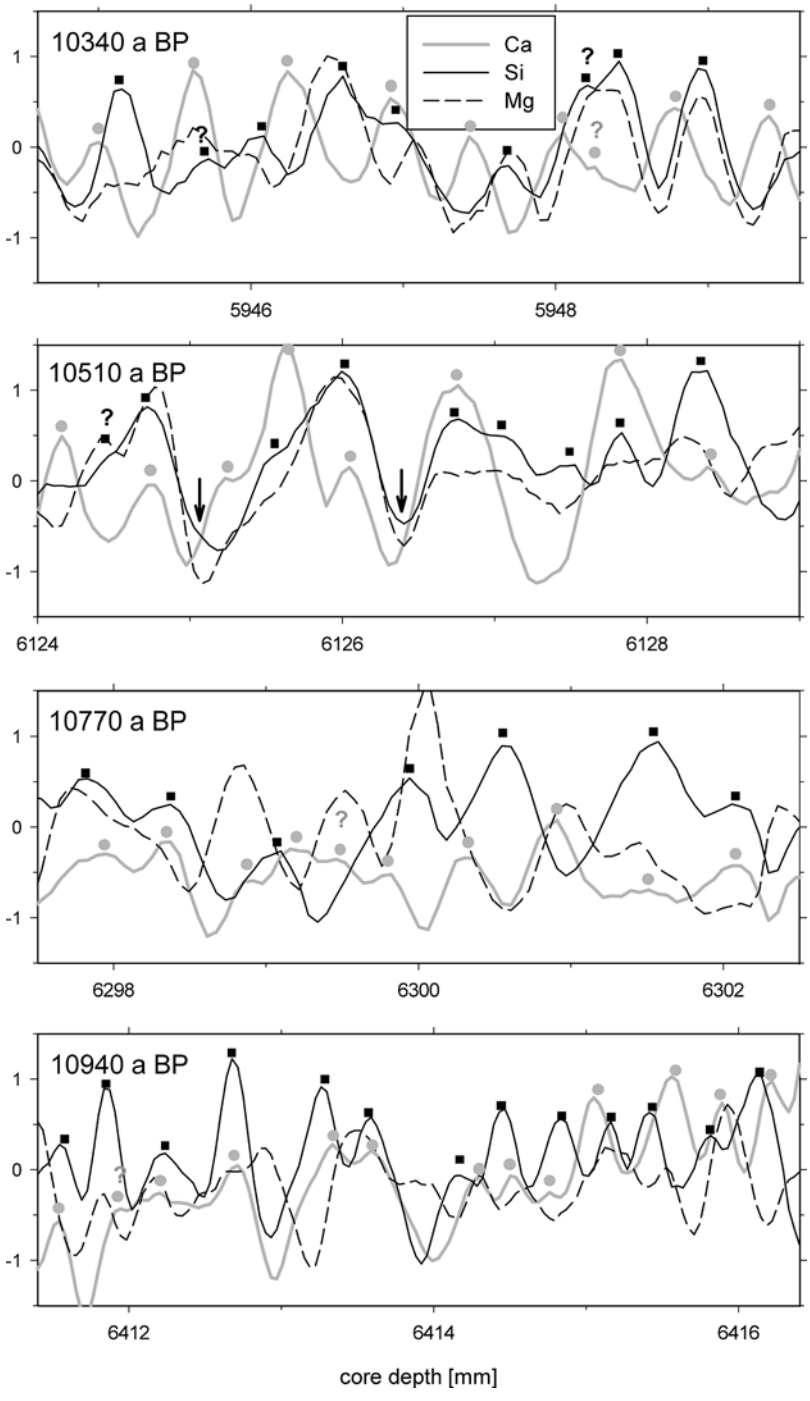

Fig. 6 Concentrations of the elements Ca, Si, and Mg in four different, 5 mm long sections *versus* core depth. Original microprobe data (counts) were standardized and smoothened by a repeated running mean over three and five values, respectively. The counted Ca and Si peaks are indicated by *circles* and *squares*, respectively. Uncertain varves are identified by question marks. Arrows in section 10,510 point to bloom years caused by partial mixing

winter. It contains fine-grained, organic carbon-rich detritus and the absence of pollen corroborates its winter origin (Lemcke 1996). Of these three laminae, the authigenic carbonate layers show the highest regularity and were used for varve counting and determination of annual accumulation rates (Landmann et al. 1996a). The thickness and relative position of the dark layer formed by organically enriched detritus shows the highest variability. In the microprobe analyses, this layer produces a minimum number of total counts because of its low content of the investigated elements.

Four sections were chosen which characterize the high variability of element distribution within the laminae of the investigated core portion. Concentrations of Si, Ca, and Mg, which are the elements with the strongest microprobe signal, are plotted in high resolution to allow interpretation of seasonal deposition differences and diagenetic processes (Fig. 6). The section 10,940* a BP represents a period with increasing Mg concentration. In the deeper part, the Si peaks follow directly the Ca peak indicating the occurrence of the river runoff maximum in winter. In the higher section, the Ca peak becomes broad and less distinct, and is covered by up to three Si peaks. The concurrent Si and Ca minima mark the position of a detritus-rich phase that is enriched in Mg. While the annual character of the Si input seems to be maintained, the Ca concentration is redistributed by diagenetic re-crystallization. X-ray diffraction analyses from this core section show diffuse reflections between 2 Θ values 30.7–32.3 interpreted as poorly crystallized protodolomite and magnesite (Landmann et al. 1996b). Formation of these minerals seems to take place predominantly within the organic detritus phase but to a certain degree also within the pore space of the lithogenic phase.

In the section 10,770* a BP, Mg enrichment reaches its maximum. Most of the time Mg and Si correlate positively in the Lake Van record, but in this period they show a distinct negative correlation. Ca concentration culminates mostly with Si and some peaks are broadened over several years as observed in the previous section. Two to four Ca maxima with low amplitudes can be bordered by sharp minima. Compared with Si-defined years, only 4 out of 5 years would be counted if relying on the Ca peaks in this period.

In the next section, centred at around 10,510* a BP, the transgression had started from a lake depth of only about 150 m (Fig. 3). This implies that the salinity may have been as high as 160 per mill (Landmann et al. 1996b). The Mg and Si content of the sediment is low during this phase (Fig. 5) but their annual peaks correlate well. The amplitude of Ca peaks varies strongly and culminates predominantly together with Si. Minima of all major elements are found frequently at the same position, indicating the presence of a pronounced organic detritus phase. This is confirmed by the high content of organic carbon within this core portion (Thiel et al. 1997). Culmination of Na at the same position (not shown) may represent remains of pore waters of high salinity since the organic matter phase has a high porosity. This pattern is interpreted to represent a meromictic phase of Lake Van. Dissolved elements like Ca will accumulate in the epilimnion since contact with the alkaline hypolimnion was prevented by a strong density gradient. Contrastingly, nutrients will accumulate within the hypolimnion due to settling and decomposition of dead biomass. Partial mixing or a complete overturn will mix the two reservoirs thus initiating enhanced $CaCO_3$ precipitation and strong plankton blooms. These mixing events seem to happen every 2–3 years (Fig. 6), leaving behind marked carbonate-rich and detritus-rich laminae. However, weaker Si and Ca signals of years without mixing are still detectable by microprobe analyses. The numbers of Si and Ca peaks are in good correspondence and reflect an increase of the accumulation rate (see also Fig. 7).

In the section centred at around 10,340* a BP, the deposition pattern finally became similar to the present condition. The Ca peaks regularly precede the minima of all major elements (i.e., the carbonate layer is separated from the organic detritus layer) and the Si peaks. The amplitudes and shapes of all peaks are more uniform and the accumulation rate is reduced. Statistical analyses of the character of the light absorption curve, as well as microprobe elemental curves prepared in some younger core sections (Landmann 1996), suggest that this pattern reflects standard lake dynamics under stable lake-level conditions and with only small density differences between upper and lower water body permitting regular, annual partial mixing of the lake.

In order to reconstruct changes in the seasonal behavior from the deposition signal in more detail, the time offset for particle sinking through the water column has to be taken into account. This requires information from the past such as grain size of the suspended matter load and water density which are not available. At any rate, it appears that the sedimentation velocity in the period covered by the investigated record did not seriously alter the deposition signal.

The next step was to use the microprobe curves to establish a refined varve chronology. However, uncertainties arise from differences in the number of Ca and Si peaks, differences between counts of parallel microprobe profiles of the same core section, or doubts regarding the annual character of elemental peaks with low intensities. Therefore, only ranges were obtained for each microprobe profile with a maximum and a minimum value. Mean values and standard deviation were calculated for all 19 microprobe profiles totalling 862±91 years. These are 166 years more compared with the varve count based on optical methods for the same core portions (696 years). There are 41.8 mm of gaps in the microprobe data in different sections; if these are included at average sedimentation rates, the total adds up to 933 years with an addition of 170 years compared to the optical count, shifting the investigated period from 10,249–11,012* a BP to 10,249–11,182 a BP.

Finally, we calculated a mean accumulation rate for each microprobe section. It is compared (Fig. 7) with the old annually resolved accumulation rate (Landmann et al. 1996a). The most pronounced difference between the two curves appears during the period when the lake level rose 10,550–10,350* a BP, and when a changed mixing

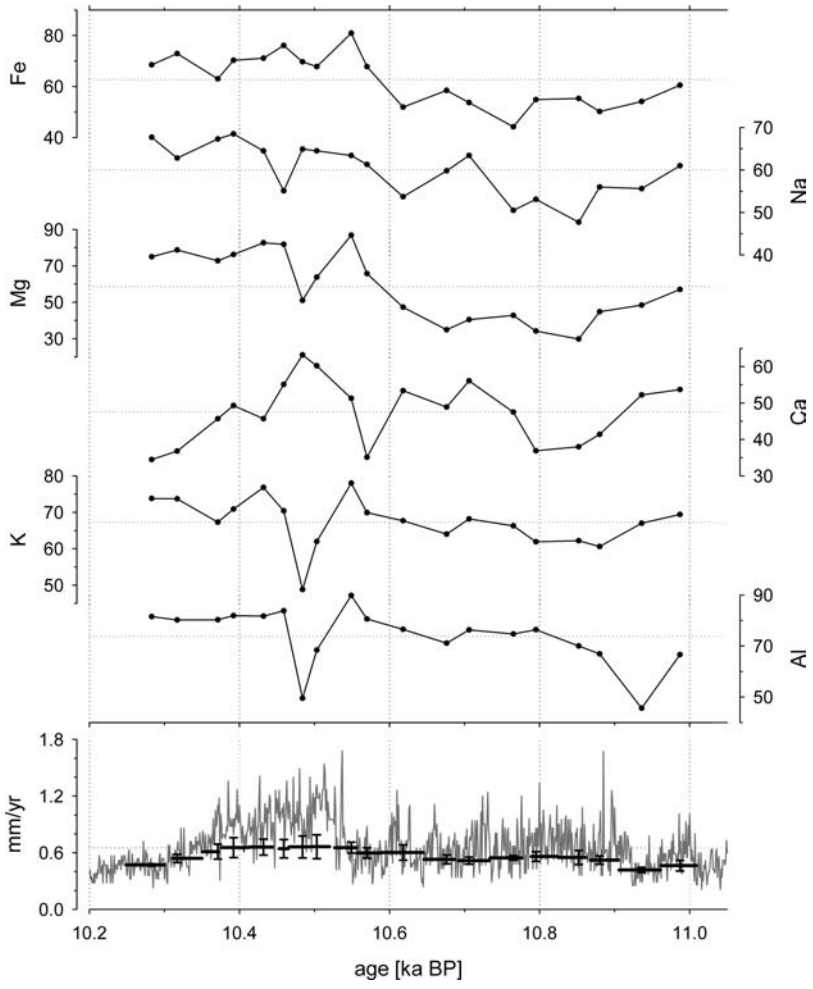

Fig. 7 Bottom: Accumulation rates for Lake Van based on microprobe analyses (bold line) compared with the previous accumulation established by automated optical methods (Landmann et al. 1996a). Error bars indicate the standard deviation of counting error within a microprobe section. Top: Synchronization of concentration gradients for six different elements relative to Si. For all elements (*y*-axis), the percentage of the gradients having the same sign as the Si gradient is given. The *x*-axis of all plots presents age according to the varve chronology prepared by Landmann (1996)

behavior of the lake masked the annual signal. Low Ca peaks are overridden by strong, simultaneously occurring inputs of terrigenous material and vice versa. Varve counts based on optical inspection detect only the grey scale value differences between these mixed signals and the prominent, dark organic rich detritus layers which are triggered by mixing events. Most of the weak, disputable peaks appear in this period, causing the highest standard deviation of the annual accumulation rate values. The optical count also failed in the periods with high Mg deposition since diagenetic carbonate formation took place within the dark, highly porous organic detritus phase and thereby weakened the differences in grey scale value between varve laminae. Only at around 10.3* ka BP, when low standard deviations of microprobe data signalize easily recognizable peaks, results of both methods begin to correlate well again.

In order to characterize temporal changes of annual deposition cycles the first derivative of the concentration, i.e., the gradients, was calculated for all elements. Gradients between adjacent data points are either positive, i.e., the concentration increases, or negative, i.e., the concentration decreases. These signs were compared with the gradient sign of Si to determine the degree of synchronization between elements (simultaneous increase or decrease; Fig. 7). The highest synchronization exists between Al and Si; on average, 74% of all Al gradients have the same sign as those of Si. The close correspondence between Al and K indicates the importance of clay minerals as constituents of Lake Van sediment. Weak gradient synchronization of both elements with Si appears around 10.5* ka BP, when Si concentration sharply rises due to higher contributions of biogenic opal.

In contrast to Al, Ca is the element showing the weakest synchronization with Si (48%); this is exactly as expected for a 'regular' seasonal sedimentation. Strong increase of synchronization between both elements starts at 10,550* a BP, simultaneous with an increasing Ca concentration (Fig. 5) and is attributed to additional Ca delivered as particulate matter together with Si. Mg synchronization has an extended minimum from 10.9 to 10.6* ka BP (i.e., during the period with high Mg content; see Fig. 5) which can be attributed to the secondary formation of Mg-carbonates.

Iron is an important indicator for the redox situation of the lake. In general, its concentration shows good correspondence with Al and K, proving that it is mainly fixed to clay minerals (Landmann 1996; Lemcke 1996). With the start of the transgression at 10.6* ka BP, physical conditions of the lake favored an oligomictic phase causing an upward shift of the redox boundary. This is expressed by

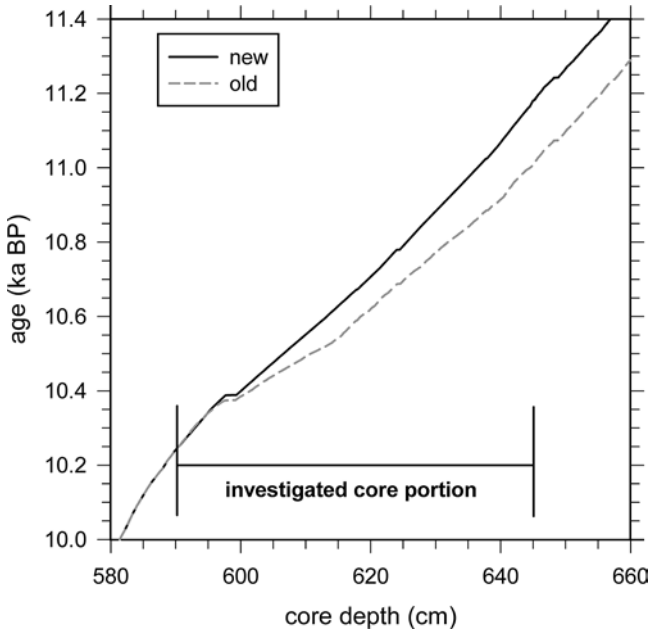

Fig. 8 Comparison of the old and new chronology of Lake Van *versus* core depth. The small plateaus in the curves indicate the presence of turbidites where core depth increases but sediment age remains unaltered. The core section between 590 and 645 cm was investigated

an increase of synchronization between Si and Fe (Fig. 7). During the regression period 11–10.6* ka BP, some of the iron may have been fixed as $FeCO_3$.

At around 15 ka BP, pronounced water-level changes have been described also for Lake Lisan, the precursor of the Dead Sea. There, unordered Mg-carbonates with comparable X-ray diffraction signals as well as diagenetic gypsum were found in the laminated sediments of the glacial terraces (Landmann et al. 2002). These diagenetic precipitates may explain differences between the chronology based on laminae counting and aragonite radiocarbon dating, the first being significantly younger (Migowski et al. 2001).

Conclusions

The present study underlines the value of microprobe analysis in those cases when varve formation may have been influenced by lake dynamics, for example caused by lake-level regression. Compared to optical methods, microprobe analysis is more sensitive and therefore a useful additional tool to investigate seasonal changes of laminated sediments; it should be particularly valuable when varve chronologies from periods of lake-level regression are used for time series analysis. The method allows interpretation of authigenic processes and detects temporal changes of river inputs or sediment porosity with high resolution.

Microprobe data and their interpretation regarding behavior of Lake Van are in good accordance with previous geochemical and sedimentological findings. They substantiate the established lake-level curve and more precisely date the start of the transgression to 10.6* ka BP. The new varve chronology adds 170 years to the old chronology based on optical varve counting. It extends the period 10,249–11,012* a BP to 10,249–11,182 a BP (Fig. 8). Within this period, grey scale value variations of lamination are weakened by the changed mixing behavior of the lake and by diagenetic processes.

The additional 170 years cover only part of the gap of 600–700 years that exists between the chronologies of Lake Van and the Greenland ice cores. To recalibrate the entire varve chronology of Lake Van, microprobe analyses are also needed for other periods of the record: From 9 to 8* ka BP, another lake-level drop occurred which also caused the formation of Mg-carbonates, thus possibly obliterating the seasonal varve signal. The same is true from 12.1 to 11* ka BP since this is the real onset of the regression investigated here. Also elevated dolomite concentrations and high deposition rates were found in this period (Landmann et al. 1996b). Obliteration of the seasonal varve signal is also expected within sediments older than 13.8* ka BP, the period when Lake Van was refilled after its complete desiccation in the Late Pleistocene.

Acknowledgments We thank B Thybusch and M Heck for their assistance during the microprobe analyses and for their patience (in spite of inadequate payment) during the optimization of the methodology. LA Melim and an anonymous reviewer improved this paper by their useful comments. This publication is a contribution to DFG projects Wo 395-4 (Lake Van) and Ke 287-16 (Lake Lisan)

References

Allen BD, Anderson RY (2000) A continuous, high-resolution record of late Pleistocene climate variability from Estancia basin, New Mexico. GSA Bull 112:1444–1458

Alley B, Meese DA, Shuman CA, Gow AJ, Taylor KC, Grootes PM, White JWC, Ram M, Waddington ED, Mayewski PA, Zielinski GA (1993) Abrupt increase in Greenland snow accumulation at the end of the Younger Dryas event. Nature 362: 527–529

Brauer A, Endres CE, Negendank JFW (1999) Lateglacial calendar year chronology based on annually laminated sediments from Lake Meerfelder Maar; Germany. Quat Int 61:17–25

Degens ET, Kurtmann F (1978) The Geology of Lake Van. MTA, Ankara, 158 pp

Grootes PM, Stuiver M, White JWC, Johnsen S, Jouzel J (1993) Comparison of oxygen isotope records from the GISP2 and GRIP Greenland ice cores. Nature 366:552–554

Kempe S (1977) Hydrographie, Warvenchronologie und organische Geochemie des Van Sees, Osttürkei. Mitt Geol-Paläont Inst Univ Hamburg 47:125–228

Kempe S, Landmann G, Müller G (2002) A floating varve chronology from the Last Glacial Maximum terrace of Lake Van/Turkey. Z Geomorph NF 126:97–114

Landmann G (1996) Van See/Türkei: Sedimentologie, Warvenchronologie und regionale Klimageschichte seit dem Spätpleistozän. PhD-Thesis, Fac Geosci Univ Hamburg, Germany, 123 pp

Landmann G, Kempe S (2002) Seesedimente als Klimaarchiv—Fallbeispiele: Van See und Totes Meer. In: Rosendahl W, Hoppe A (eds) Angewandte Geowissenschaften in Darmstadt. Schriftenr Dt Geol Ges 15:129–143

Landmann G, Reimer A, Lemcke G, Kempe S (1996a) Dating Late Glacial abrupt climate changes in the 14,570 yr long continuous varve record of Lake Van, Turkey. Palaeogeogr Palaeoclimatol Palaeoecol 122:107–118

Landmann G, Reimer A, Kempe S (1996b) Climatically induced lake level changes at Lake Van, Turkey, during the Pleistocene/Holocene transition. Global Biogeochem Cycles10:797–808

Landmann G, Abu Qudaira GM, Shawabkeh K, Wrede V, Kempe S (2002) Geochemistry of Lisan and Damya Formations in Jordan and implications for palaeoclimate. Quat Int 89:45–57

Langbein WB (1961) Salinity and hydrology of closed lakes. Geol Surv Prof Pap 412:20

Lemcke G (1996) Paläoklimarekonstruktion am Van See (Ostanatolien, Türkei). PhD-Thesis, ETH Zürich, Switzerland, 182 pp

Litt T, Brauer A, Goslar T, Merkt J, Balaga K, Müller H, Ralska-Jasiewiczowa M, Stebich M, Negendank JFW (2001) Correlation and synchronization of lateglacial continental sequences in northern central Europe based on annually laminated lacustrine sediments. Quat Sci Rev 20:1233–1249

Migowski C, Prasad S, Negendank JFW, Stein M (2001) Pleistocene-Holocene sediments from Lake Lisan and Dead Sea. Contr EUG Abstr, Strasbourg, 8–12 April 2001, p 763

Neev D, Emery KO (1967) The Dead Sea. Depositional Processes and Environments of Evaporites. Geol Surv Israel Bull 41: 147 pp

Neev D, Emery KO (1995) The destruction of Sodom, Gomorrah, and Jericho: geological, climatological, and archaeological background. Oxford Univ Press, Oxford, 175 pp

Reimer A (1995) Hydrochemie und Geochemie der Sedimente und Porenwässer des hochalkalinen Van Sees in der Osttürkei. PhD-Thesis, Univ Hamburg, Germany, 123 pp

Talbot MR, Lærdal T (2000) The late Pleistocene-Holocene palaeolimnology of Lake Viktoria, East Africa, based upon elemental and isotopic analyses of sedimentary organic matter. J Paleolimnol 23:141–164

Thiel V, Jenisch A, Landmann G, Reimer A, Michaelis W (1997) Unusual distributions of long-chain alkenones and tetrahydrahymanol from the highly alkaline Lake Van. Turkey. Geochim Cosmochim Acta 61:2053–2064